# Deletion of STK40 Protein in Mice Causes Respiratory Failure and Death at Birth[*][S]

**Hongyao Yu**[‡§1], **Ke He**[¶1], **Lingjie Li**[‡2], **Lei Sun**[‡3], **Fan Tang**[¶], **Ruizhen Li**[¶4], **Wen Ning**[‖], and **Ying Jin**[‡§5]

*From the* ‡*Key Laboratory of Stem Cell Biology, Institute of Health Sciences, Shanghai Institutes for Biological Sciences, Chinese Academy of Sciences/Shanghai JiaoTong University School of Medicine, 225 South Chongqing Road, Shanghai 200025, China, the* ¶*Laboratory of Molecular Developmental Biology, Institute of Medical Sciences, Shanghai JiaoTong University School of Medicine, Shanghai 200025, China,* ‖*College of Life Sciences, Nankai University, Tianjin 300071, China, and the* §*University of the Chinese Academy of Sciences, Beijing 100049, China*

**Background:** STK40 is a putative serine/threonine kinase. Little is known about its physiological function.
**Results:** STK40 deletion causes fetal lung immaturity and neonatal death with altered expression of genes important for lung development.
**Conclusion:** STK40 is required for alveolar epithelium maturation and function.
**Significance:** Discovery of the role of STK40 in lung maturation helps to understand the molecular regulation in lung development.

STK40 is a putative serine/threonine kinase and was shown to induce extraembryonic endoderm differentiation from mouse embryonic stem cells. However, little is known about its physiological function *in vivo*. Here, we generate *Stk40* knock-out mice and demonstrate that loss of the *Stk40* gene causes neonatal lethality at birth. Further examination reveals that the respiratory distress and atelectasis occur in the homozygous mutants. The maturation of lung and alveolar epithelium is delayed in the mutant, as indicated by narrowed air spaces, thickened interstitial septa, and increased glycogen content in the lungs of *Stk40*^{−/−} mice. The reduction in levels of T1-α, SP-B, and SP-C indicates delayed maturation of both type I and type II respiratory epithelial cells in *Stk40*^{−/−} lungs. Moreover, *Stk40* is found to be most highly expressed in lungs of both fetal and adult mice among all organs tested. Mechanistically, a genome-wide RNA microarray analysis reveals significantly altered expression of multiple genes known to participate in lung development. The expression of some genes involved in lipid metabolism, immune response, and glycogen metabolism is also disrupted in the lung of *Stk40*^{−/−} mice. Protein affinity purification identifies RCN2, an activator of ERK/MAPK signaling, as an STK40-associated protein. Consistently, *Stk40* deficiency attenuates the ERK/MAPK activation, and inhibition of ERK/MAPK activities reduces surfactant protein gene expression in lung epithelial cells. Collectively, this study uncovers an important role of STK40 for lung maturation and neonatal survival. STK40 may associate with RCN2 to activate ERK/MAPK signaling and control the expression of multiple key regulators of lung development.

In mammals, the placenta provides gas exchange in the fetus solely. At birth, the transition from an aqueous to air breathing environment takes place. The process is entirely dependent on the normal structure and function of the lung, which provides large surface areas for exchange of oxygen and carbon dioxide. Both structurally and functionally, the lung is divided into two distinct parts, the proximal airway for conducting air and the peripheral airways for mediating gas exchange (1). At the late stage of gestation, fetal lung undergoes alveolarization, a process of peripheral alveolar epithelial cells to differentiate into mature squamous type I alveolar epithelial cells (AEC-I)[6] and secretory cuboidal type II alveolar epithelial cell (AEC-II) bearing lamellar bodies that contain surfactants. Morphologically, there is continued remodeling of distal lung, involving expansion of presumptive alveoli, thinning of the mesenchyme, and extensive growth of the capillary network into close position to respiratory epithelial cells (2, 3). The surfactant proteins and lipids are required for reducing surface tension at the air-liquid interface after birth. Their synthesis and secretion are key factors in determining whether the newborn lung can sustain gas exchange without collapsing. The immaturity in the peripheral lung and resultant deficiency in the pulmonary surfactant complex lead to respiratory distress syndrome, a leading cause of death in preterm birth of mammals, including humans (4).

Lung morphogenesis is precisely instructed by the coordination of numerous intrinsic transcription factors and extracellu-

lar signaling pathways. Transcription factors, such as TTF-1 (thyroid transcription factor 1; Nkx2.1), NFIb, C/EBPα (CCAAT/enhancer-binding protein α), GATA-6, β-catenin, Foxa1, and HNF3b (Foxa2), have been shown to play important roles in the regulation of genes and processes required for the respiratory function of the lung at birth (5–12). Signaling pathways, including those associated with FGFs (fibroblast growth factors), Shh (sonic hedgehog), BMP4 (bone morphogenetic protein 4), VEGFs, members of the Wnt (wingless-type MMTV integration site) family, Ptc (patched receptor), Smo (smoothened), and the Glis, have also been implicated in the complex interactions among different cell types in the lung (13–19). Despite extensive studies on the lung morphogenesis and function, the important genes involved in the molecular regulation of lung formation and function are not fully identified and characterized. A better understanding of the precise temporal and spatial control of cell proliferation, migration, and differentiation in the developing lung is critical for researchers to design more effective strategies to treat lung diseases, especially for neonatologists.

The *Stk40* (serine/threonine kinase 40) gene encodes a 435-amino acid protein with a conserved serine/threonine kinase domain. Its sequence orthologs have been found in a number of other organisms (20). Our previous study found that STK40 could activate the ERK/MAPK signaling pathway through its interaction with RCN2, a $Ca^{2+}$-binding protein, in mouse embryonic stem cells. Forced expression of *Stk40* induced the extraembryonic endoderm differentiation from mouse embryonic stem cells (20). However, the physiological roles of STK40 in late gestation and adulthood are barely known. In the current study, we generated *Stk40* knock-out (*Stk40$^{-/-}$*) mice through homologous recombination and found that *Stk40$^{-/-}$* mice died shortly after birth. Further study revealed that *Stk40$^{-/-}$* mice had substantially reduced peripheral alveolar expansion before birth and failed to initiate breathing at birth. At a molecular level, the expression of some important genes associated with maturation of respiratory epithelial cells was disrupted by the deficiency of *Stk40*. Comparison of genome-wide gene expression profiles between lungs of *Stk40* wild-type (*Stk40$^{+/+}$*) and knock-out mice provides insights into the molecular mechanism by which STK40 might contribute to fetal lung development and function.

## EXPERIMENTAL PROCEDURES

*Animal Husbandry and Genotyping*—*Stk40$^{+/-}$* mice were generated at the Model Animal Research Center of Nanjing University (MARC). Homologous recombination was accomplished by substitution of the second and third exons of the *Stk40* gene with the *Escherichia coli* β-galactosidase (*lacZ*) gene. All animals were raised in the specific pathogen-free facility, and procedures were performed according to the guidelines approved by the Shanghai JiaoTong University School of Medicine. Genotypes were determined by Southern blot analysis (conducted by MARC) and genomic PCR with specific primers targeting the *Stk40* gene or exogenous *lacZ* gene. Primers were as follows: for *Stk40*, forward (5′-GCTCGAGTCAGGAACAC-TGTT-3′) and reverse (5′-TACAGGAGGCTCAGGGAAA-TAC-3′); for *lacz*, forward (on targeting vector) (5′-AGCAGC-

CATGTGATGTATCC-3′) and reverse (on *lacZ sequence*) (5′-AACTGTTGGGAAGGACGATC-3′).

*Morphological Analyses*—Tissues from fetal and neonatal lungs for light microscopic examination were fixed in 4% paraformaldehyde overnight at 4 °C. For the paraffin section, tissues were then gradually dehydrated and embedded in paraffin. Five-μm sections were prepared and stained with hematoxylin and eosin solution or immunostained by antibodies. ProSP-C, T1-α, and TTF-1 proteins were detected by anti-proSP-C (FL197, Santa Cruz Biotechnology, Inc.), T1-α (M172, Santa Cruz Biotechnology, Inc.) or TTF-1 (H190, Santa Cruz Biotechnology, Inc.) antibodies, respectively, following the instructions of the standard DAB staining kit (Zhongshanjinqiao, Beijing, China). For frozen sections, tissues were dehydrated with 30% sucrose overnight and embedded in O.C.T (Sakura Finetek). Ten-μm sections were prepared and stained with anti-proSP-C antibody and then Cy3-conjugated secondary antibody for immunofluorescence staining.

*BrdU Incorporation Assay*—Cellular proliferation in the lungs of E18.5 embryos was measured by nuclear incorporation of BrdU as previously reported (21). Unconjugated AffiniPure Fab fragment goat anti-mouse IgG (H + L) was used to block endogenous mouse IgG (115-007-003, Jackson Immuno-Research Laboratories) for 1 h at room temperature before primary antibody application. Quantitative measurement was made with FV10 ASW software (Olympus Micro). The lung mass areas were measured with Adobe Photoshop CS. Five random fields at a magnification of ×10 were selected from each sample. Relative positive cells/area was normalized to one wild-type sample (set as 1). The images were taken under the identical exposure setting.

*TUNEL Assay*—Tissue sections were deparaffinized, rehydrated, and stained using the Apoptag peroxidase *in situ* apoptosis detection kit (S7100, Millipore) according to the manufacturer's instructions. The relative number of positive cells/area was calculated as described under "BrdU Incorporation Assay."

*Western Blotting*—Total proteins from the fetal lung were extracted with 0.1% SDS-radioimmune precipitation assay buffer or 62.5 mM Tris-HCl (pH 6.7). Protein quantification was made with the BCA method (Pierce). Proteins were blotted on the PVDF or nitrocellulose membrane and visualized using rabbit polyclonal antibodies of T1-α (M172, Santa Cruz Biotechnology, Inc.), SP-B (H300, Santa Cruz Biotechnology, Inc.), or SP-C at a 1:200 dilution in 3% bovine serum albumin (Sigma). Mouse monoclonal antibody of α-tubulin (Sigma) was used at a 1:2000 dilution by 5% skim milk. The Western blot quantification was performed with ImageJ software (National Institutes of Health).

*Periodic Acid-Schiff Staining*—Tissue frozen sections were stained using the periodic acid-Schiff staining kit (Hongqiaolexiang Inc., Shanghai, China) according to the manufacturer's procedure. Glycogens were shown as red deposits.

*Cell Culture and Retroviral Overexpression or RNA Interference*—Mouse embryonic fibroblasts (MEFs) were generated from E13.5 embryos and cultured in DMEM containing 10% fetal bovine serum (FBS). Murine lung epithelium cell line MLE-12 was cultured in DMEM/F-12 containing 2% FBS. The

*GFP* or *Stk40* gene was inserted into the pMXs vector, a gift from Toshio Kitamura (Tokyo University). The small RNA interference sequence for *Stk40* (Si, GGACCCATCGGATA-ACTAT) or for control (Ci, GTGCGCTGCTGGTGCCAAC) was inserted into the pSiren-RetroQ vector, a gift from Gang Wang (Shanghai Institutes for Biological Sciences, Chinese Academy of Sciences). The MLE-12 cell line was provided by Yuehai Ke (Zhejiang University, China). After 48 or 60 h of viral infection, proteins or RNAs were extracted as described above. Retroviral particles were prepared in the Plat-E cell system as reported previously (22). Viral supernatants in the same volume were used to infect primary MEFs or MLE-12 cells. The infection lasted for 10 h without selection. Before cell harvest, MEK inhibitor U0126 (Merck) dissolved in DMSO (10 $\mu$M) was added to cell culture for 12 h.

*Primary Fetal Lung Epithelial Cell Isolation*—Epithelial cells and lung fibroblast cells were isolated from fetal lungs simultaneously at E16.5 using collagenase and differential plating on cell culture dishes as described previously (23). Two days later, after isolation, cells were lysed for further tests.

*GST Pull-down Assay*—GST or GST-STK40 proteins were expressed in *E. coli* and purified according to the manufacturer's instructions (GE Healthcare). The pull-down assay was performed as previously reported (20). Eluted proteins were sent for LS/MS analysis to the Core Facility for Proteomics Technology in the Institute of Biochemistry and Cell Biology (Shanghai Institutes for Biological Sciences, Chinese Academy of Sciences). The acquired LS/MS spectra were searched using a Mascot version 2.2.2 search engine against the Mouse International Protein Index sequence database (version 3.87). All output results were combined together using in-house software named BuildSummary to delete the redundant data. The results were filtered by a minimum score of 25.

*RNA Extraction and RT-PCR Analysis*—Total RNA was extracted using TRIzol reagent (Invitrogen) according to the manufacturer's instructions. Expression levels of marker genes were quantified by quantitative real-time RT-PCR (qRT-PCR) (HT7900). Primers were as follows: *Gapdh*, forward (5′-GTC-GTGGAGTCTACTGGTGTC-3′) and reverse (5′-GAGCCC-TTCCACAATGCCAAA-3′); *Stk40*, forward (5′-GCAAGGA-ATAGAGAGCCAAG-3′) and reverse (5′-TACCATCC-GACCAGACTCTG-3′); *SP-A*, forward (5′-GAGGAGCTTC-AGACTGCACTC-3′) and reverse (5′-AGACTTTATCCCCC-ACTGACAG-3′); *SP-B*, forward (5′-GGCTGTGTCCCAGG-TGTGCC-3′) and reverse (5′-AGGCTCCACAGCAG-GGAGGG-3′); *SP-C*, forward (5′-TAGCCCCGAGTGAGCG-AGCA-3′) and reverse (5′-GTGGGTGTGGAGGGCTTGGC-3′); *SP-D*, forward (5′-GCCTGGTCGTGATGGACGGG-3′) and reverse (5′-AGGGCCCTGCAACCCTGAGA-3′); *T1-α*, forward (5′-CAGGAGACGGCATGGTGCCC-3′) and reverse (5′-AGGCTTCGTCCCACGCTCTCT-3′); *TTF-1*, forward (5′-CATGGGCAAGGGTCAGGGGC-3′) and reverse (5′-GCC-TGGCCCTGTCTGTACGC-3′); *CC-10* (Clara cell protein 10), forward (5′-GCGGGCACCCAGCTGAAGAG-3′) and reverse (5′-GAGCCGAGGAGACACAGGGCA-3′). Primers for microarray data verification were as follows: *SP-A*, forward (5′-AGGCAGACATCCACACAGCTT-3′) and reverse (5′-ACTTGATGCCAGCAACAACAGT-3′); *SP-B*, forward (5′-

CATTTATCAGCGGAGACAGCAAG-3′) and reverse (5′-AGAGCCATTTACTGCCTACTCGG-3′); *SP-C*, forward (5′-CGCCAAAGCAAAGAGTGAAACG-3′) and reverse (5′-TTTACCCCACCTTCTCCCACAC-3′); *SP-D*, forward (5′-ACGTGGACTAAGTGGACCTCC-3′) and reverse (5′-CCT-TTTGCCCCTGTAGATCCTT-3′); *T1-α*, forward (5′-TGCT-ACTGGAGGGCTTAATGA-3′) and reverse (5′-TGCTGAG-GTGGACAGTTCCT-3′); *CC-10*, forward (5′-CATGCT-GTCCATCTGCTGC-3′) and reverse (5′-CTCTTGTGGGA-GGGTATCC-3′); *GR* (glucocorticoid receptor), forward (5′-AGCTCCCCCTGGTAGAGAC-3′) and reverse (5′-GGTGA-AGACGCAGAAACCTTG-3′); *HGF*, forward (5′-GGCAAG-GTGACTTTGAATGA-3′) and reverse (5′-CACATGGTCC-TGATCCAATC-3′); *FGF-18*, forward (5′-CCTGCACTTG-CCTGTGTTTAC-3′) and reverse (5′-TGCTTCCGACTCAC-ATCATCT-3′); *Shh*, forward (5′-GAGCAGACCGGCTGAT-GACT-3′) and reverse (5′-ACAGAGATGGCCAAGGCATT-3′); *FGF-1*, forward (5′-CAGCTCAGTGCGGAAAGTG-3′) and reverse (5′-ATAAAAGCCCTTCGGTGTCCA-3′); *Pref-1* (*Dlk-1*) (preadipocyte factor 1/δ-like 1 homolog (*Drosophila*)), forward (5′-AGCCCTCCTGCGCGTCCTCTT-3′) and reverse (5′-GAATTTCCCGTCCCAGCCATCCTT-3′); *KLF-4* (Kruppel-like factor 4), forward (5′-GTGCCCCGACTAACC-GTTG-3′) and reverse (5′-GTCGTTGAACTCCTCGGTCT-3′); *KLF-5*, forward (5′-ACCTCCGTCCTATGCCGCTAC-3′) and reverse (5′-TCCGGGTTACTCCTTCTGTTGT-3′); *C/EBPα*, forward (5′-GTGTGCACGTCTATGCTAAACCA-3′) and reverse (5′-GCCGTTAGTGAAGAGTCTCAGTTTG-3′); *Wnt2*, forward (5′-CTCGGTGGAATCTGGCTCTG-3′) and reverse (5′-CACATTGTCACACATCACCCT-3′).

*RNA Microarray Analyses*—Total lung RNA was isolated as described above to prepare three *Stk40*$^{+/+}$ and three *Stk40*$^{-/-}$ samples, respectively. Each sample contained pooled RNA from four lungs at E18.5. Three biological replicates for each genotype were then prepared and hybridized to the Affymatrix mouse 430 2.0 array by the Shanghai Biochip Company (SBC). Gene ontology clustering was analyzed by the SBC analysis system and online DAVID Bioinformatics Resources (24).

*Statistic Analysis*—All results were analyzed with the Sigma-Plot version 10.0 program. Data are presented as the mean ± S.D. Student's *t* test was used to compare differences between two groups with at least three independent experiments or samples.

## RESULTS

*Targeted Disruption of the Stk40 Locus Causes Neonatal Lethality*—We designed a *Stk40* gene-targeting vector that replaced the second and third exons in the N-terminal sequence of *Stk40* gene with the *E. coli lacZ* gene and a stop codon to fully disrupt *Stk40* gene expression (Fig. 1*A*). Homologous recombination of gene targeting in embryonic stem cells of the 129 strain was verified by Southern blot analyses using DNA probes located in the 5′- or 3′-flanking region of the *Stk40* gene (Fig. 1, *A* and *B*). Embryonic stem cells with one of the *Stk40* alleles deleted were used to create chimeras and further develop a stable heterozygous mouse strain. The mice were then back-crossed with C57/B6J mice for more than 10 generations. The genotype of fetuses was determined by genomic
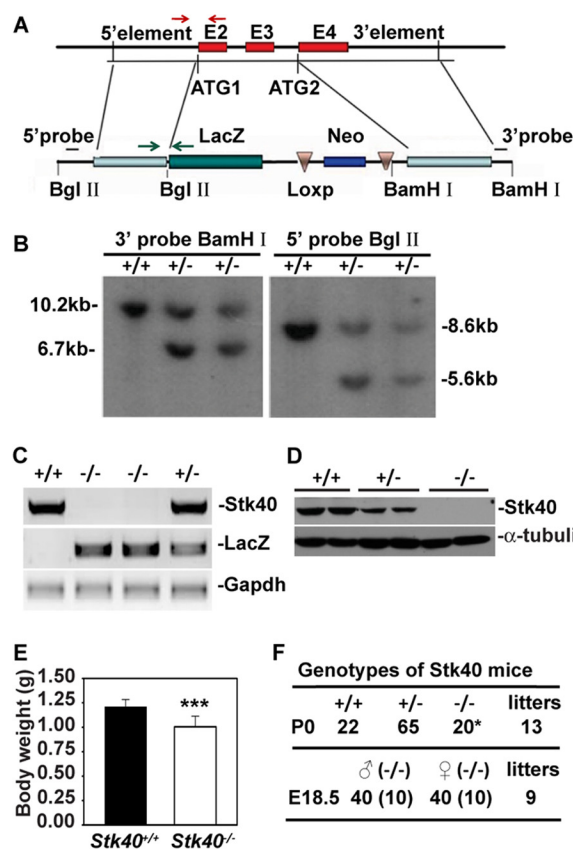
FIGURE 1. **Targeted disruption of the *Stk40* locus in mice leads to death at birth.** *A*, diagram of the targeting vector used to generate *Stk40* knock-out mice, showing the flanking arms of 5′- and 3′-elements. The *lacZ* gene and loxped Neo cassette were cloned into the targeting vector. *Red* and *green arrows* indicate the sequences of primers for *Stk40* and *lacZ* genotyping, respectively. *B*, Southern blot for genotyping using genomic DNA of embryonic stem cells, which were digested with BamHI or BglII and probed with the 3′- or 5′-probe, respectively. The wild-type and heterozygous clones are shown. *C*, genomic PCR to determine the genotypes of mice with specific primers. *Gapdh* was used as a DNA loading control. *D*, Western blot for genotyping using total proteins of an E18.5 lung tissue. $\alpha$-Tubulin was used as a loading control. *E*, a comparison of the body weight of E18.5 C-sectioned mice between *Stk40*$^{+/+}$ and *Stk40*$^{-/-}$ pups. *Stk40*$^{+/+}$, *n* = 14; *Stk40*$^{-/-}$, *n* = 13. ***, *p* < 0.001. *F*, a summary of the genotype for newborn or C-sectioned pups. The *asterisk* indicates that some dead fetuses might be missed, probably due to maternal cannibalism. +/+, wild type; +/−, heterozygote; −/−, knockout. ♂ (−/−), male (knock-out male); ♀ (−/−), female (knock-out female). *Error bars*, S.D.

PCR with specific primers and Western blot analysis against STK40 protein (Fig. 1, *C* and *D*).

Heterozygous *Stk40*$^{+/-}$ mice were alive and healthy as their normal littermates. They did not display any discernable abnormalities in the development, growth, and reproduction. However, we did not obtain any homozygous mutants that survived for more than 12 h during normal delivery (E19.5–E21). Among 107 pups born, 20 died within 12 h or were found dead. All of the *Stk40*$^{-/-}$ pups had significantly reduced body weight and size as compared with their littermates (Fig. 1*E*). To exclude the maternal cannibalism influence, we delivered the pups before their natural birth (E18.5). The genotype of all offspring was consistent with the Mendelian inheritance and was not sexually biased (Fig. 1*F*). Therefore, we drew the conclusion that *Stk40* is an essential gene for the survival of mice at birth.

*Respiratory Failure Occurs in Stk40$^{-/-}$ Mice*—We found that *Stk40*$^{-/-}$ mice had difficulties breathing at birth. They
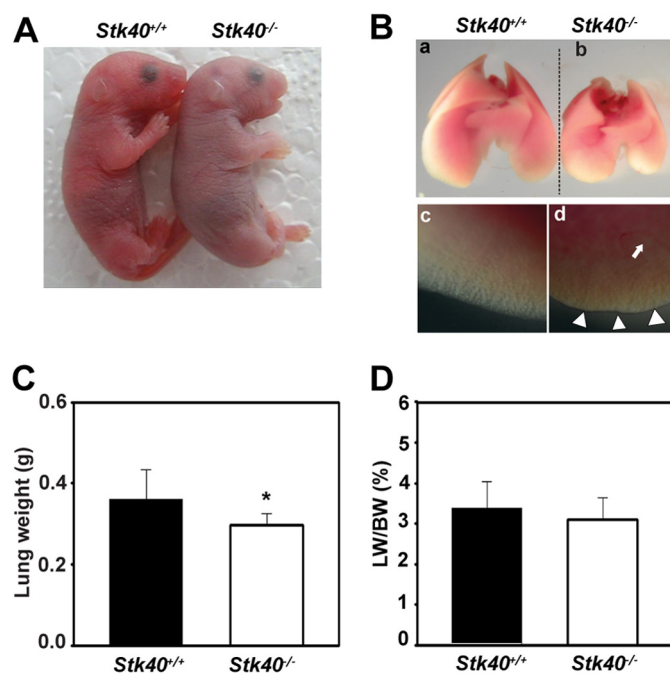


FIGURE 2. ***Stk40* knock-out results in pulmonary atelectasis.** *A*, a photograph of P0 pups. *B*, bright views of E18.5 lungs. Compared with the normally developed lung in *Stk40*$^{+/+}$ mice (*a* and *c*), the *Stk40*$^{-/-}$ lung was smaller in size (*b*), with the fissure (*white arrow* in *d*) being insufficiently expanded peripherally (*white arrowheads* in *d*). *C*, a comparison of the lung weight of E18.5 mice. *Stk40*$^{+/+}$, *n* = 14; *Stk40*$^{-/-}$, *n* = 7. *, *p* < 0.05. *D*, a comparison of the lung weight/body weight ratio (*LW/BW*). *Stk40*$^{+/+}$, *n* = 4; *Stk40*$^{-/-}$, *n* = 7. *Error bars*, S.D.

made deep respiratory movements involving the whole-body muscles immediately after birth but failed in initiating normal breathing (supplemental Movie 1). *Stk40*$^{-/-}$ mice turned cyanotic and only survived for a few h, suggesting that these pups suffered from respiratory distress (Fig. 2*A*). The respiratory movement observed in *Stk40*$^{-/-}$ mice excluded neuromuscular or muscular dysfunctions as causes for their respiratory failure.

When lungs of *Stk40*$^{-/-}$ fetuses at E18.5 were examined grossly, evidently small sized and poorly expanded lobes with fissures could be found, although the shape and number of lobes appeared normal (Fig. 2*B*). Moreover, the weight of lungs of homozygous mutants was significantly lower than that of wild-type mice (Fig. 2*C*), whereas there was no difference when the ratio of lung weight and body weight was compared (Fig. 2*D*). These observations suggested that lung development and respiratory failure might contribute to the death of *Stk40*$^{-/-}$ mice.

*Maturation of Lungs Is Delayed in Stk40$^{-/-}$ Mice*—The histological examination of *Stk40*$^{+/+}$ lungs at P0 displayed normal saccular expansion and thin septa. By contrast, substantially reduced alveolar space and thicker interstitial mesenchymal compartments were observed in the lungs of *Stk40*$^{-/-}$ mice. There were extensive pulmonary atelectasis and congestion in lungs of the *Stk40*$^{-/-}$ corpses, whereas no typical hyaline membrane formation was found (Fig. 3*A*). At E18.5, both AEC I and AEC II cells should line the peripheral saccules, which is the typical mature structure of the lung at this stage of gestation. As expected, we observed many properly inflated small distal sac-
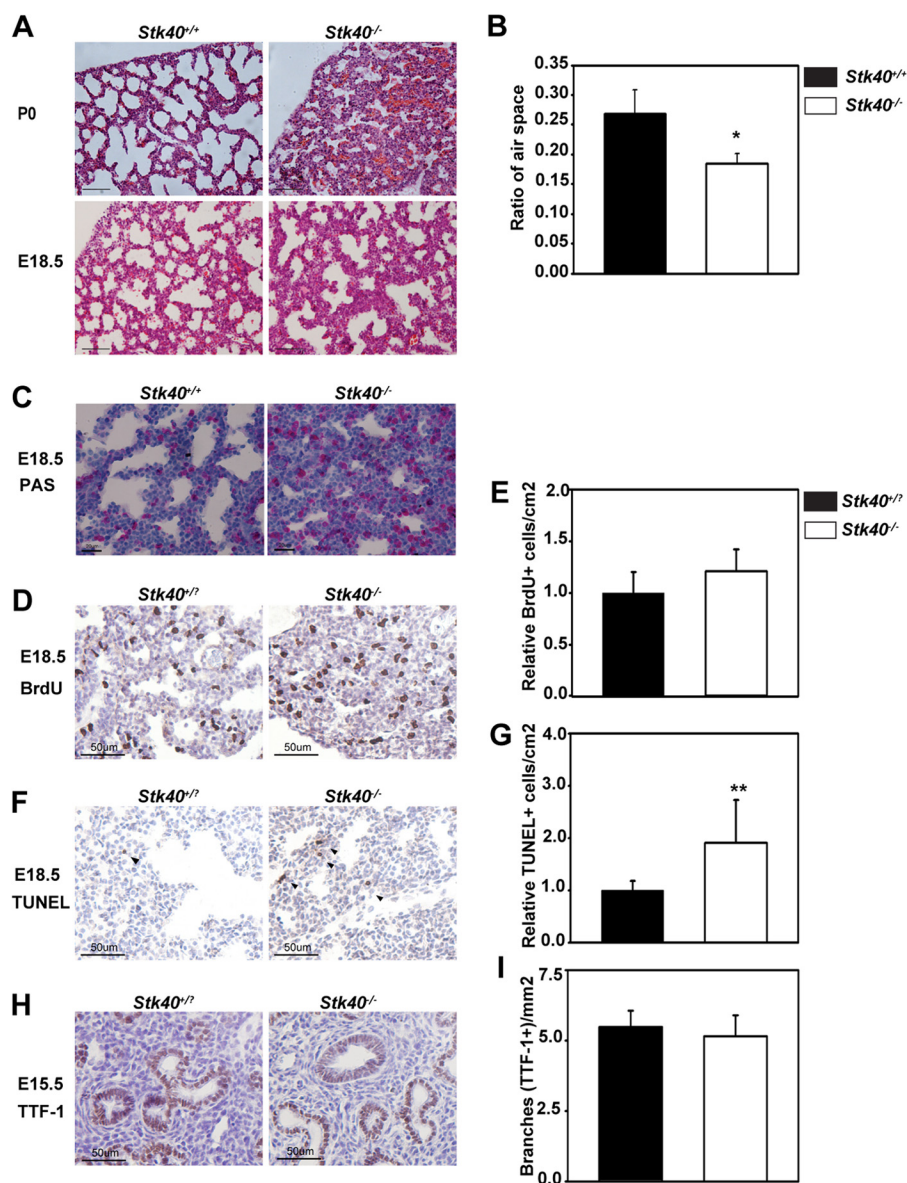
FIGURE 3. **Fetal lungs are immature in $Stk40^{-/-}$ mice.** *A*, hematoxylin and eosin staining of $Stk40^{+/+}$ and $Stk40^{-/-}$ lungs of P0 and E18.5 mice. *Scale bars*, 50 $\mu$m. Three lungs for each genotype were serially sectioned and compared. Representative results are shown. *B*, ratio of air space in lungs of E18.5 mice. The *numbers* indicate the ratio of air space area and the total lung area of sections. $Stk40^{+/+}$, $n = 7$; $Stk40^{-/-}$, $n = 3$. *C*, periodic acid-Schiff staining of E18.5 lungs. The *red color* indicates the glycogen deposit. *Scale bars*, 20 $\mu$m. Three lungs for each genotype were serially sectioned and compared. Representative results are shown. *D*, BrdU staining of E18.5 lungs. Nuclei were counterstained with hematoxylin. *Scale bars*, 50 $\mu$m. $Stk40^{+/?}$ indicates wild-type or heterozygous mice. *E*, quantification of BrdU-positive cells. All data were normalized to one corresponding wild-type level (set as 1). $Stk40^{+/?}$, $n = 7$; $Stk40^{-/-}$, $n = 5$. *F*, TUNEL staining of E18.5 lungs. Nuclei were counterstained with hematoxylin. *Scale bars*, 50 $\mu$m. *Arrowheads* indicate the positive cells. *G*, quantification of TUNEL-positive cells. All data were normalized to one corresponding wild-type level (set as 1). $Stk40^{+/?}$, $n = 9$; $Stk40^{-/-}$, $n = 7$. *H*, immunohistochemistry (*IHC*) staining of TTF-1 in paraffin sections of E15.5 lungs. *Scale bars*, 50 $\mu$m. *I*, quantitative analysis of TTF-1-positive branches. All data were normalized to one corresponding wild-type level (set as 1). $Stk40^{+/?}$, $n = 3$; $Stk40^{-/-}$, $n = 3$. *, $p < 0.05$; **, $p < 0.01$. *Error bars*, S.D.

cules in the $Stk40^{+/+}$ lung. In contrast, the dilation was severely impaired with thicker septa in the $Stk40^{-/-}$ lung (Fig. 3*A*). The ratio of the air space was significantly lower in $Stk40^{-/-}$ lungs than in $Stk40^{+/+}$ lungs (Fig. 3*B*), implying that the maturation of lungs in $Stk40^{-/-}$ fetuses may be delayed. Moreover, we examined the level of glycogen in lungs of E18.5 mice because the enrichment in glycogen is one of the features of immature AEC II cells (25). Periodic acid-Schiff staining of sections of $Stk40^{-/-}$ lungs showed an increased level of glycogen as a *red deposit* (Fig. 3*C*), further supporting the idea that deletion of $Stk40$ causes the immaturity of the fetal lung.

*Deletion of Stk40 Does Not Affect Cell Proliferation but Increases Apoptotic Cells at the Late Gestation Stage*—To determine the causes of hypoplasia observed in $Stk40^{-/-}$ lungs, we examined the cell proliferation and apoptosis through BrdU incorporation and TUNEL assays, respectively. The density of BrdU$^+$ cells was comparable between lungs of wild-type and knock-out mice at E18.5 (Fig. 3, *D* and *E*), suggesting that cell proliferation at this stage in the lung was not affected by the deletion of $Stk40$. However, TUNEL staining results showed that the density of apoptotic cells in the lungs of $Stk40^{-/-}$ mice was 2-fold higher than that in the wild-type lungs at E18.5 (Fig. 3, *F* and *G*).
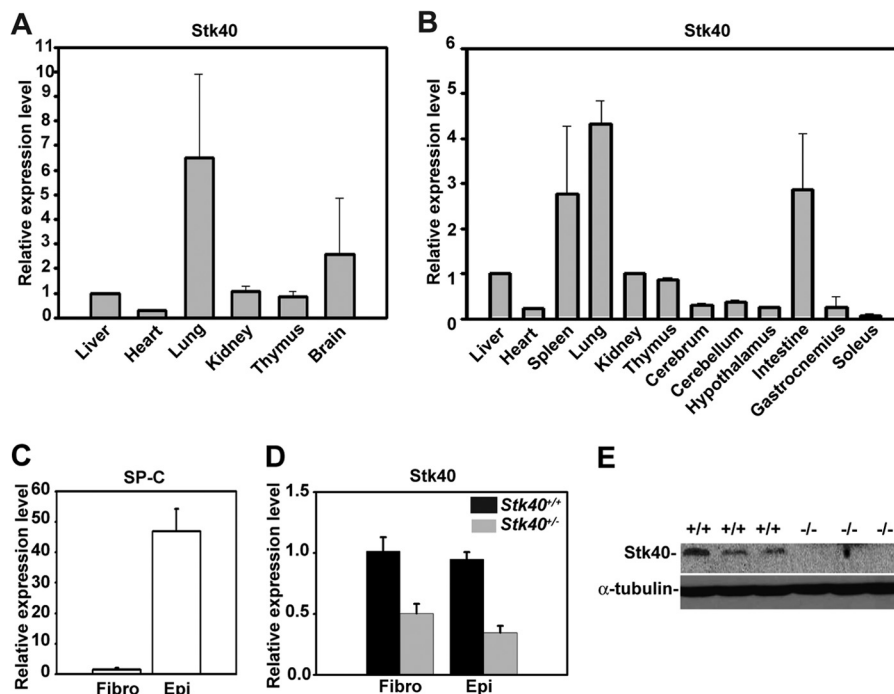
FIGURE 4. **STK40 is most highly expressed in fetal and adult lungs.** *A*, the relative expression level of *Stk40* in fetal organs was determined by qRT-PCR. All data were normalized to the liver expression level with *Gapdh* as an internal control. Organs from six mice were pooled together for each experiment, and the experiment was repeated three times independently. *B*, the relative expression level of *Stk40* in adult organs was examined by qRT-PCR. All data were normalized to liver expression with *Gapdh* as an internal control. RNA was extracted from organs of female mice at 6–8 weeks old. *n* = 3. *C*, relative expression level of *SP-C* in primary lung epithelial cells isolated from E16.5 embryos by qRT-PCR. The expression level of *SP-C* in lung fibroblasts was set as 1. *n* = 3. *D*, relative expression level of *Stk40* in lung epithelial and fibroblast cells. The expression level of *Stk40* in one wild-type sample was set as 1. *Stk40*$^{+/+}$, *n* = 3; *Stk40*$^{+/-}$, *n* = 3. *E*, Western blotting of STK40 expression in fetal lung epithelial cells. *Error bars*, S.D.

We also examined the cell proliferation and cell apoptosis in fetal lungs at E15.5 because pulmonary cells proliferate, and the airway branches quickly to form the entire respiratory tree at this stage of development. Apoptotic cells were hardly detected for either *Stk40*$^{+/+}$ or *Stk40*$^{-/-}$ lungs, and similar BrdU$^+$ cell densities were found in lungs of both genotypes at E15.5 (data not shown). In addition, we found that TTF-1, which marks all epithelial cells in the lung, displayed a similar branching pattern between *Stk40*$^{-/-}$ and control lungs (Fig. 3, *H* and *I*). Thus, *Stk40* deficiency did not produce evident defects in the lung until E15.5. The cell apoptosis caused by *Stk40* deletion at the late stage of lung development could at least partially contribute to the lung hypoplasia.

*Stk40 Is Highly Expressed in the Lungs of Fetal and Adult Mice*—The above data indicate that STK40 plays an important role in lung development. We were interested in knowing whether it was expressed in lungs during development. Due to the lack of a good antibody for STK40 immunostaining, qRT-PCR analysis was employed to compare the expression level of *Stk40* among different organs. Interestingly, *Stk40* was most highly expressed in the lung in both fetal (E18.5) and adult (6–8 weeks) mice among all organs tested (Fig. 4, *A* and *B*). At E18.5, the lung was the only organ highly expressing *Stk40* (Fig. 4*A*). Low levels of *Stk40* transcripts were detected in the liver, heart, kidney, thymus, and brain of E18.5 fetuses. At adulthood, relatively high levels of *Stk40* were also found in the spleen and intestine, despite the level being lower than in the lungs. In the other adult organs tested, *Stk40* transcript levels were low (Fig. 4*B*). The *Stk40* expression pattern reinforces the conclusion

that *Stk40* is a critical gene associated with fetal lung development before birth and also lung function after birth.

To learn in which cell types *Stk40* was expressed in the lung, we isolated primary lung epithelial cells from E16.5 embryos and examined the expression of *Stk40* in these lung epithelial cells and simultaneously isolated fibroblast cells. The lung epithelial identity of isolated epithelial cells was verified by the higher level of *SP-C* in the epithelial cells than in the lung fibroblast cells (Fig. 4*C*). Lung epithelial and fibroblast cells expressed *Stk40* at a similar level (Fig. 4*D*). As expected, the expression level of *Stk40* in *Stk40*$^{+/-}$ cells was about half of that in *Stk40*$^{+/+}$ cells (Fig. 4*D*). In addition, we detected STK40 proteins in the *Stk40*$^{+/+}$ epithelial cells but not in *Stk40*$^{-/-}$ cells (Fig. 4*E*), further validating the expression of STK40 in lung epithelial cells. These data clearly show that lung epithelial cells and fibroblasts express *Stk40*, hinting at potential functions of *Stk40* in these cells.

*Expression of Alveolar Epithelial Differentiation Markers Is Altered in Stk40*$^{-/-}$ *Lungs*—Pulmonary alveolar epithelial cells express specific genes marking their cell identity and maturation. For instance, AEC II cells produce surfactant proteins (SP-A, SP-B, SP-C, and SP-D), which are required for respiratory initiation or lung defense. Disrupted expression of SP-B and SP-C proteins could lead to severe respiratory distress in newborn infants (26–29). We found that, in lungs of E18.5 *Stk40*$^{-/-}$ mice, mRNA levels of *SP-A*, *SP-B*, and *SP-C* decreased, whereas the level of *SP-D* increased (Fig. 5*A*). Consistently, protein levels of prosurfactant proteins (proSP-B and proSP-C) in *Stk40*$^{-/-}$ lungs were lower than in *Stk40*$^{+/+}$ lungs,
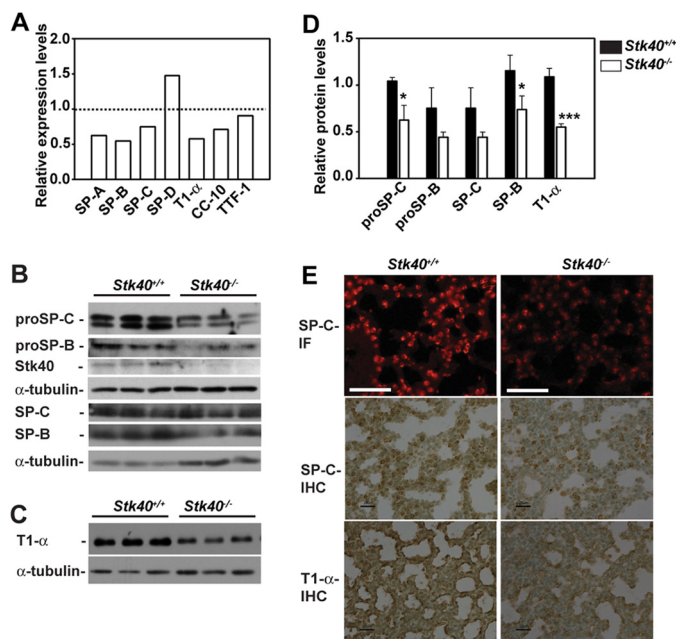
FIGURE 5. **The expression of alveolar epithelial cell differentiation markers is altered in $Stk40^{-/-}$ lungs.** A, relative expression levels of lung cell differentiation markers were determined by qRT-PCR. All data were normalized to corresponding wild-type levels (set as 1) with *Gapdh* as an internal control. Data shown are the mean values of two independent experiments. Each experiment utilized pooled RNA extracted from six $Stk40^{+/+}$ or $Stk40^{-/-}$ lungs of the same litters, respectively. *Dotted line*, gene expression levels in wild-type lungs. B, Western blotting of SP-B, SP-C (including prosurfactant proteins and mature surfactant proteins), and STK40 of individual lungs. C, Western blotting of T1-$\alpha$ of individual lungs. D, quantification of the Western blotting results shown in B and C. All samples were measured by ImageJ and normalized to one wild-type level (set as 1) with $\alpha$-tubulin as an internal control. *, $p < 0.05$; ***, $p < 0.001$. E, immunofluorescence (*IF*) staining of SP-C in frozen sections of E18.5 lungs (*top*). *Scale bars*, 50 $\mu$m. *Middle*, Immunohistochemistry (*IHC*) staining of SP-C in paraffin sections of E18.5 lungs. *Scale bars*, 20 $\mu$m. *Bottom*, immunohistochemistry staining of T1-$\alpha$ in paraffin sections of E18.5 lungs. *Scale bars*, 20 $\mu$m. $Stk40^{+/+}$, $n = 6$; $Stk40^{-/-}$, $n = 7$. Representative results are shown. *Error bars*, S.D.

as indicated by results from both Western blot and immunostaining analyses, suggesting that AEC II cells could not differentiate normally in the absence of *Stk40* (Fig. 5, B and C). Particularly, the mature form of SP-B also decreased, which often results in the failure of breathing initiation. We also examined the expression of the AEC I cell differentiation marker T1-$\alpha$. Results from qRT-PCR, Western blotting, and immunostaining analyses all indicated a remarkable reduction in the expression of T1-$\alpha$ in $Stk40^{-/-}$ lungs (Fig. 5, A, D, and E). In addition, we detected lower expression of *CC-10*, a non-ciliated secretory cell bronchial marker, in $Stk40^{-/-}$ lungs (Fig. 5A). Nevertheless, the mRNA level of transcription factor *TTF-1*, a master gene for lung development, was comparable between lungs of two different genotypes (Fig. 5A). Taken together, the reduced expression of genes associated with fetal lung maturation indicates that deletion of *Stk40* delayed the maturation of pulmonary epithelial cells and compromised the function of the lung, which may in turn lead to the lung atelectasis.

*STK40 Regulates Expression Profiles of Multiple Genes Involved in Lung Development*—To identify the genes influenced by the deletion of *Stk40* in the lung at a genome-wide scale, transcriptomes of E18.5 lungs were compared between $Stk40^{+/+}$ and $Stk40^{-/-}$ mice using the Affymatrix mouse 430
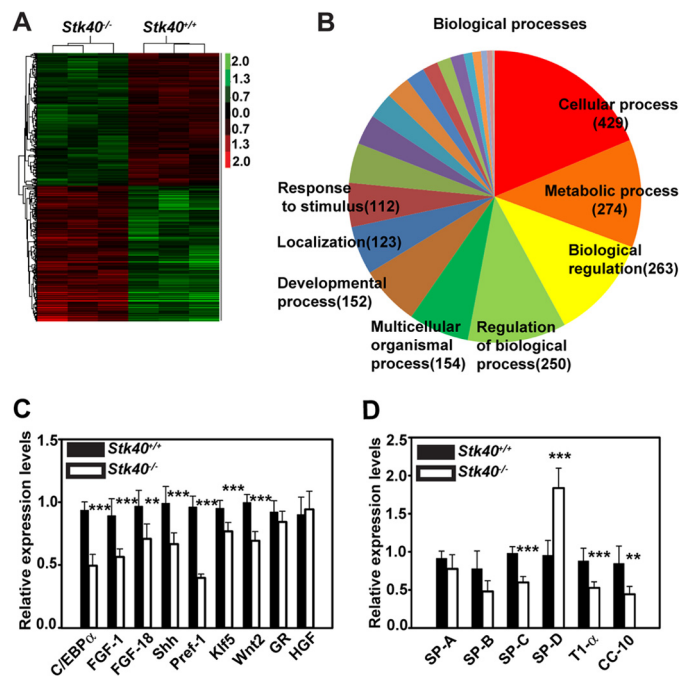


FIGURE 6. **STK40 regulates the expression of important genes associated with lung development.** A, the heat map of DEGs in the lungs ($p < 0.05$, 1.5-fold or more) between $Stk40^{+/+}$ and $Stk40^{-/-}$ mice. B, a pie chart of gene ontology clustering for the DEGs shown in A. C, verification of some DEGs identified in microarray analyses by qRT-PCR analyses. Total RNA was extracted from lungs of E18.5 fetuses. $Stk40^{+/+}$, $n = 6$; $Stk40^{-/-}$, $n = 6$. D, verification of epithelial cell differentiation marker expression in E18.5 lungs by qRT-PCR analyses. $Stk40^{+/+}$, $n = 6$; $Stk40^{-/-}$, $n = 6$. *, $p < 0.05$; **, $p < 0.01$; ***, $p < 0.001$. *Error bars*, S.D.

2.0 array. Microarray analysis identified 931 probe sets (763 genes) that were significantly altered by 1.5-fold or more in $Stk40^{-/-}$ lungs ($p < 0.05$) (Fig. 6A). Among them, levels of 319 genes were decreased and 444 genes were increased in $Stk40^{-/-}$ lungs. Gene ontology enrichment analyses of the differentially expressed genes (DEGs) revealed that the large proportion of DEGs was involved in cellular processes, metabolic processes, biological regulation, multicellular organismal processes, and developmental processes (Fig. 6B). Specifically, 30 DEGs have been known to be involved in lung or respiratory development, such as *T1-$\alpha$*, *SP-D*, *FGF-18*, *FGF-1*, *C/EBP$\alpha$*, *Shh*, *Wnt2*, etc. In line with the microarray data, our qRT-PCR analysis verified the reduced expression of *FGF-18*, *FGF-1*, *Shh*, *C/EBP$\alpha$*, *KLF4*, *KLF5*, *Pref-1* (*Dlk-1*), and *Wnt2* in $Stk40^{-/-}$ lungs (Fig. 6C). Deficiency in the expression of some of these genes has been reported to cause severe lung defects and neonatal lethality (11, 18, 30–33). As a negative control, there was no significant difference in the expression of *GR* and *HGF* based on data from both microarray and qRT-PCR analyses. Unexpectedly, microarray analysis did not identify genes encoding surfactant proteins (SP-A, SP-B, and SP-C) as DEGs, whereas results of our earlier qRT-PCR analysis indicated a reduction in the expression of these genes (Fig. 5A). To clarify the inconsistency between the two assays, we conducted qRT-PCR experiments again, utilizing new sets of primers and newly collected lung samples. As a result, mRNA levels of all three genes were lower in $Stk40^{-/-}$ lungs than in $Stk40^{+/+}$ lungs, although only the difference in the *SP-C* level was statistically significant (Fig. 6D). Together with the consistent results for other genes
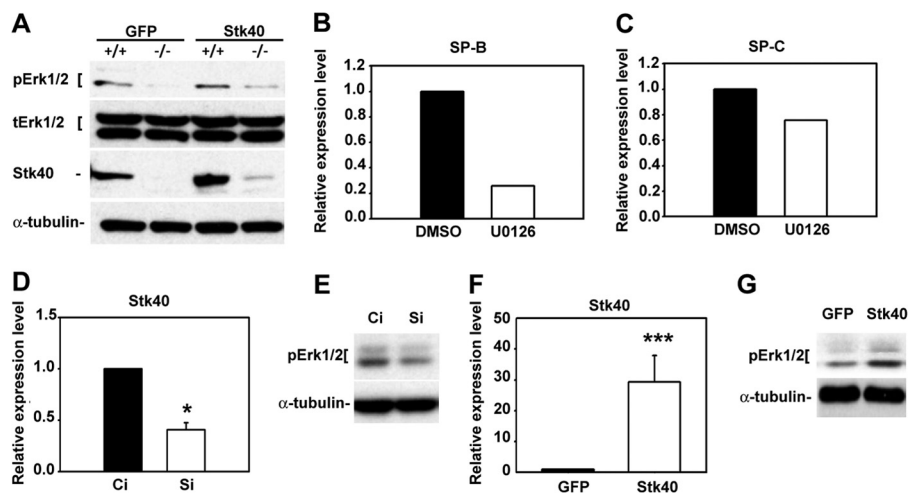
FIGURE 7. **STK40 regulates the ERK/MAPK activity in lung epithelial cells.** *A*, Western blotting analysis of the ERK/MAPK activity in MEFs. *pErk1/2* and *tErk1/2*, active ERK1/2 and total ERK1/2, respectively. $\alpha$-Tubulin was used as a loading control. *GFP* or *Stk40* was overexpressed in the MEFs by retroviral infection. *B* and *C*, relative expression levels of surfactant proteins SP-B and SP-C in MLE-12 cells with or without U0126 treatment. DMSO was used as a vehicle control. Data shown are the mean values of two independent experiments. *D*, the mRNA level of *Stk40* after infection of retroviral vector-mediated *Stk40* RNA interference in MEL-12 cells. *Ci* and *Si*, control and *Stk40* RNA interference, respectively. *, $p < 0.05$. *E*, Western blotting of active ERK1/2 in control or *Stk40* RNA interference vector-infected MLE-12 cells. $\alpha$-Tubulin was used as a loading control. *F*, the mRNA level of *Stk40* after infection of retroviral vector-mediated *Stk40* overexpression in MLE-12 cells. *GFP* was used as control. ***, $p < 0.001$. *G*, Western blotting of active ERK1/2 in *GFP*- or *Stk40*-overexpressing MLE-12 cells. $\alpha$-Tubulin was used as a loading control. *Error bars*, S.D.

obtained from microarray and qRT-PCR analyses, we believe that results from both assays are reliable. It appears that qRT-PCR is a more sensitive analysis to confirm DEGs, whereas microarray has the advantage of detecting DEGs at a genome-wide scale.

In addition, microarray data revealed that the genes encoding molecules regulating lipid metabolism and transporter activity (*FABP4*, *Abcb1a*, *Abcb1b*, *PPAR*$\gamma$, *Pref-1*, *Apoe*, etc.), glycogen metabolism and biosynthesis (*St3gal1*, *St8sia6*, *Fut4 Fut10*, etc.), inflammatory response and host defense (*SP-D*, *Hc*, *Ccl1*, *Ccl2*, *Ccl3*, *Ccl4*, *Ccl13*, *Ccr5*, *Tlr4*, *Tlr5*, *Pf4*, *Ha-Aa*, *MR1*, etc.), and antioxidant and complement (*Iyd*, *Ptgs2*, *Txnerd3*, *C1qa*, *C1qb*, *C6*, etc.) were significantly increased or decreased in the lungs of *Stk40*$^{-/-}$ mice. Collectively, altered expression of these molecules involved in lung maturation and function would lead to pulmonary defects observed in *Stk40*$^{-/-}$ mice.

*STK40 May Regulate Surfactant Protein Expression through ERK/MAPK Activation*—In an effort to understand how STK40 regulates expression of the genes associated with lung development, we carried out GST-STK40 fusion protein-based affinity purification using whole-cell lysate proteins extracted from MEF cells, followed by a mass spectrometric analysis. GST proteins were used as a negative control for the purification. Interestingly, RCN2 was identified (supplemental Table 1). Among the identified potential partners of STK40, we were particularly interested in RCN2, an intracellular $Ca^{2+}$-binding protein (34). It was previously shown to interact directly with STK40 and to be required for STK40 to activate Ras-Raf-ERK1/2 signaling in mouse embryonic stem cells (20). Furthermore, the ERK/MAPK pathway was also found to be pivotal for fetal lung cell growth, survival, and branching morphogenesis (35, 36). At adulthood, the FGF/ERK/SPs cascade is known to function in lung repair after injury (37, 38). In addition, our microarray data indicated a reduction in the expression levels for *FGF-1*, *FGF-4*, and *FGF-18* as well as other factors involved in the ERK/MAPK

pathway, such as Pref-1, in *Stk40*$^{-/-}$ lungs. We anticipated that STK40 might control lung epithelial differentiation and maturation through association with RCN2 to activate ERK/MAPK signaling. Supporting the hypothesis, we found that phosphorylation levels of ERK1/2 in *Stk40*$^{-/-}$ MEF cells were markedly lower than in *Stk40*$^{+/+}$ cells. Reintroduction of STK40 could recover ERK1/2 phosphorylation levels in *Stk40*$^{-/-}$ cells (Fig. 7A), indicating a critical role of STK40 in the ERK1/2 activity. Moreover, inhibition of the ERK/MAPK signaling by its specific inhibitor U0126 substantially reduced the expression of *SP-C* and *SP-B* in lung epithelial MLE-12 cells (Fig. 7, *B* and *C*). Consistent with previous reports (36, 38), our finding argues for an important role of ERK/MAPK signaling for the production of surfactant proteins. To further verify the link between STK40 and the ERK/MAPK signaling in lung epithelial cells, the expression of *Stk40* was silenced in MLE-12 cells using retroviral vector-mediated RNA interference (Fig. 7D). Knockdown of *Stk40* reduced the phosphorylation level of ERK1/2 (Fig. 7E). In contrast, overexpression of *Stk40* enhanced the ERK/MAPK activity in MLE-12 cells (Fig. 7, *F* and *G*). Taken together, these results indicate that STK40 plays a conserved role in the activation of the ERK/MAPK pathway, probably through its direct interaction with RCN2, regulating the expression of surfactant protein and other lung development-associated genes.

## DISCUSSION

The neonatal breathing difficulty is one of the major disorders causing preterm infant mortality (39). Tremendous efforts have been made to identify important genes controlling lung development and functions in order to better understand the coordination of signaling pathways and transcriptional networks regulating the lung morphogenesis as well as to develop more effective strategies of respiratory distress treatment (2, 19). Here, we show that STK40 is crucial for perinatal lung maturation and initiation of respiration. A number of experi-

mental results obtained in this study support this conclusion as follows. 1) Deletion of *Stk40* led to lethal respiratory failure at birth. *Stk40*$^{-/-}$ pups attempted to breathe, but they looked cyanotic and died soon after delivery. 2) Lungs of *Stk40*$^{-/-}$ pups were not adequately inflated. Air spaces in peripheral lungs of *Stk40*$^{-/-}$ mice were dramatically reduced with thickened mesenchyme-derived stroma compared with normally expanded air saccules in *Stk40*$^{+/+}$ lungs. There were collapsed alveolar structure and congestion in the lungs of *Stk40*$^{-/-}$ mice. The phenotype resembles the newborn respiratory distress, although hyaline membrane formation was not observed. 3) Deletion of *Stk40* disrupted respiratory epithelial cell differentiation. Low levels of surfactant proteins, particularly SP-B and SP-C, as well as the higher level of glycogen deposits in lungs of *Stk40*$^{-/-}$ mice indicate compromised differentiation of AEC II cells. Deletion of *SP-B* was shown to generate lethal respiratory failure, which could not be compensated for by increased expression of *SP-D* (40). Moreover, the low level of T1-$\alpha$ in *Stk40*$^{-/-}$ lungs suggests disrupted differentiation of AEC I cells. The expression of *CC-10*, a gene expressed by Clara cells, also decreased in *Stk40*-deleted lungs. Combined with the finding that *Stk40* is most highly expressed in the lungs among other mouse organs examined during the terminal saccular phase (E17 to term), it is clear that STK40 is required for fetal lung maturation and epithelial cell differentiation. As a result, deletion of *Stk40* gave rise to compromised epithelial cell differentiation and reduced synthesis of surfactant proteins, subsequently leading to respiratory failure and neonatal lethality in mice. Nevertheless, we cannot absolutely exclude the possibility that defects in other tissues or organs contributed to the neonatal atelectasis observed in *Stk40* null mice.

It is important to understand how STK40 participated in lung development. To this end, we conducted a genome-wide transcriptome analysis of *Stk40*$^{+/+}$ and *Stk40*$^{-/-}$ lungs at E18.5. Microarray data analyses revealed altered expression of many marker genes of pulmonary epithelial cells. For example, the mRNA level of *T1-$\alpha$* was found to be lower in *Stk40*$^{-/-}$ lungs than in *Stk40*$^{+/+}$ lungs. Further experiments of qRT-PCR, Western blotting, and immunostaining validated the reduction in T1-$\alpha$ in *Stk40*$^{-/-}$ lungs. T1-$\alpha$ is the AEC I integral membrane glycoprotein and is relatively specifically expressed in alveolar AEC I cells during embryonic lung development. Similar to *Stk40* deficiency, homozygous *T1-$\alpha$* null mice die at birth of respiratory failure, and their lungs cannot be inflated to full volumes. Furthermore, due to the lack of T1-$\alpha$ proteins, AEC I cell differentiation is blocked, whereas differentiation of AEC II epithelial cells and the levels of surfactant proteins are normal in *T1-$\alpha$*-deleted lungs (30). Different from *T1-$\alpha$* deletion, the maturation of AEC II epithelial cells was also compromised in *Stk40*$^{-/-}$ lungs, suggesting that additional factors would be responsible for AEC II cell phenotypes. Searching carefully into DEGs between *Stk40*$^{+/+}$ and *Stk40*$^{-/-}$ lungs, we found reduced expression of a number of genes in *Stk40*-deleted lungs, which are known to be associated with maturation or function of the lung in late gestation, such as *C/EBP$\alpha$*, *FGF-1*, *FGF-18*, and *Wnt2*. However, the expression of *GR*, *TTF-1*, and *HGF* was not influenced by *Stk40* deletion, despite their important roles in lung development (7, 10, 41, 42). Loss of *C/EBP$\alpha$*

results in immaturity of AEC II pneumocytes and the absence of AEC I cells (11, 31), whereas deletion of *FGF-18* can influence distal lung remodeling at the late embryonic stage (18, 43). Wnt2 and Shh are even more critical in the regulation of lung progenitor specification and left-right branching morphogenesis (32, 33). In addition, we detected a moderate but significant reduction in the expression of *KLF5*, the loss of which inhibits the maturation of both conducting and peripheral airways (44). Of note, the changes in expression levels of these genes in *Stk40*$^{-/-}$ lungs were moderate but consistent and statistically significant. The lung phenotype of *Stk40*$^{-/-}$ mice appears not perfectly matched with any of the phenotypes produced by the complete loss of these genes. Therefore, STK40 may execute its function in fetal lungs, together with other lung development regulators, through controlling a specific set of lung development-associated genes. Its deletion causes disrupted expression of these lung development-associated genes but not their entire loss. However, the net outcome of these changes gives rise to fatal respiratory failure.

Another important unsolved issue is how STK40 controls the expression of lung development-associated genes. Identification of protein partners is one of the useful strategies to elucidate the molecular mechanism underlying the function of a particular gene. Our GST-STK40 fusion protein-based affinity purification uncovered RCN2 as an STK40-associated protein. In fact, RCN2 was previously identified and clearly demonstrated as a direct downstream mediator for STK40 to activate ERK/MAPK signaling in mouse embryonic stem cells (20). In the present study, the link of STK40 to ERK/MAPK signaling was further strengthened by intimate correlation between the phosphorylation level of ERK1/2 and STK40 expression levels in both MEF and lung epithelial cells. Therefore, the STK40-RCN2 complex might be an important activator for ERK/MAPK signaling regardless of the cell types. Functionally, ERK/MAPK signaling has been reported to play important roles in the very early stage of lung development (E12). Although the ERK/MAPK activity decreases after E12, it still plays roles in lung branching morphogenesis, lung cell proliferation, and apoptosis. Our observation that inhibition of ERK1/2 signaling reduced expression levels of SP-B and SP-C in lung epithelial cells indicates that this pathway is also important for pulmonary epithelial maturation at the late stage of lung development.

In summary, we provide experimental evidence that STK40 is an important player for the initiation of breath and survival of neonatal mice. In its absence, the maturation of pulmonary epithelial cells and synthesis of surfactant proteins were disturbed, leading to respiratory failure. Microarray data showed that STK40 regulated a number of important genes required for lung development. Altered expression of these genes could be responsible for the development of respiratory failure observed in *Stk40*$^{-/-}$ mice. Mechanistically, STK40 formed a protein complex with RCN2 to activate ERK/MAPK signaling, which in turn controlled expression of key regulators and effectors of lung development. The findings obtained in this study help us to better understand the regulation of fetal lung development and epithelial cell maturation.

## REFERENCES

1. Ten Have-Opbroek, A. A. (1991) Lung development in the mouse embryo. *Exp. Lung Res.* **17,** 111–130
2. Cardoso, W. V. (2001) Molecular regulation of lung development. *Annu. Rev. Physiol.* **63,** 471–494
3. Burri, P. H. (1984) Fetal and postnatal development of the lung. *Annu. Rev. Physiol.* **46,** 617–628
4. Avery, M. E., and Mead, J. (1959) Surface properties in relation to atelectasis and hyaline membrane disease. *AMA J. Dis. Child* **97,** 517–523
5. Minoo, P., Su, G., Drum, H., Bringas, P., and Kimura, S. (1999) Defects in tracheoesophageal and lung morphogenesis in Nkx2.1(−/−) mouse embryos. *Dev. Biol.* **209,** 60–71
6. Kimura, S., Ward, J. M., and Minoo, P. (1999) Thyroid-specific enhancer-binding protein/thyroid transcription factor 1 is not required for the initial specification of the thyroid and lung primordia. *Biochimie* **81,** 321–327
7. Lazzaro, D., Price, M., de Felice, M., and Di Lauro, R. (1991) The transcription factor TTF-1 is expressed at the onset of thyroid and lung morphogenesis and in restricted regions of the foetal brain. *Development* **113,** 1093–1104
8. Wongtrakool, C., Malpel, S., Gorenstein, J., Sedita, J., Ramirez, M. I., Underhill, T. M., and Cardoso, W. V. (2003) Down-regulation of retinoic acid receptor α signaling is required for sacculation and type I cell formation in the developing lung. *J. Biol. Chem.* **278,** 46911–46918
9. Tichelaar, J. W., Wert, S. E., Costa, R. H., Kimura, S., and Whitsett, J. A. (1999) HNF-3/forkhead homologue-4 (HFH-4) is expressed in ciliated epithelial cells in the developing mouse lung. *J. Histochem. Cytochem.* **47,** 823–832
10. Bohinski, R. J., Di Lauro, R., and Whitsett, J. A. (1994) The lung-specific surfactant protein B gene promoter is a target for thyroid transcription factor 1 and hepatocyte nuclear factor 3, indicating common factors for organ-specific gene expression along the foregut axis. *Mol. Cell Biol.* **14,** 5671–5681
11. Martis, P. C., Whitsett, J. A., Xu, Y., Perl, A. K., Wan, H., and Ikegami, M. (2006) C/EBPα is required for lung maturation at birth. *Development* **133,** 1155–1164
12. Bachurski, C. J., Yang, G. H., Currier, T. A., Gronostajski, R. M., and Hong, D. (2003) Nuclear factor I/thyroid transcription factor 1 interactions modulate surfactant protein C transcription. *Mol. Cell Biol.* **23,** 9014–9024
13. Samakovlis, C., Hacohen, N., Manning, G., Sutherland, D. C., Guillemin, K., and Krasnow, M. A. (1996) Development of the *Drosophila* tracheal system occurs by a series of morphologically distinct but genetically coupled branching events. *Development* **122,** 1395–1407
14. Min, H., Danilenko, D. M., Scully, S. A., Bolon, B., Ring, B. D., Tarpley, J. E., DeRose, M., and Simonet, W. S. (1998) Fgf-10 is required for both limb and lung development and exhibits striking functional similarity to *Drosophila* branchless. *Genes Dev.* **12,** 3156–3161
15. Bellusci, S., Grindley, J., Emoto, H., Itoh, N., and Hogan, B. L. (1997) Fibroblast growth factor 10 (FGF10) and branching morphogenesis in the embryonic mouse lung. *Development* **124,** 4867–4878
16. Warburton, D., Schwarz, M., Tefft, D., Flores-Delgado, G., Anderson, K. D., and Cardoso, W. V. (2000) The molecular basis of lung morphogenesis. *Mech. Dev.* **92,** 55–81
17. Villavicencio, E. H., Walterhouse, D. O., and Iannaccone, P. M. (2000) The sonic hedgehog-patched-gli pathway in human development and disease. *Am. J. Hum. Genet.* **67,** 1047–1054
18. Usui, H., Shibayama, N., Ohbayashi, N., Konishi, M., Takada, S., and Itoh, N. (2004) Fgf18 is required for embryonic lung alveolar development. *Biochem. Biophys. Res. Commun.* **322,** 887–892
19. Kaplan, F. (2000) Molecular determinants of fetal lung organogenesis. *Mol. Genet. Metab.* **71,** 321–341
20. Li, L., Sun, L., Gao, F., Jiang, J., Yang, Y., Li, C., Gu, J., Wei, Z., Yang, A., Lu, R., Ma, Y., Tang, F., Kwon, S. W., Zhao, Y., Li, J., and Jin, Y. (2010) Stk40 links the pluripotency factor Oct4 to the ERK/MAPK pathway and controls extraembryonic endoderm differentiation. *Proc. Natl. Acad. Sci. U.S.A.* **107,** 1402–1407
21. Geng, Y., Dong, Y., Yu, M., Zhang, L., Yan, X., Sun, J., Qiao, L., Geng, H., Nakajima, M., Furuichi, T., Ikegawa, S., Gao, X., Chen, Y. G., Jiang, D., and Ning, W. (2011) Follistatin-like 1 (Fstl1) is a bone morphogenetic protein (BMP) 4 signaling antagonist in controlling mouse lung development. *Proc. Natl. Acad. Sci. U.S.A.* **108,** 7058–7063
22. Morita, S., Kojima, T., and Kitamura, T. (2000) Plat-E. An efficient and stable system for transient packaging of retroviruses. *Gene Ther.* **7,** 1063–1066
23. Rice, W. R., Conkright, J. J., Na, C. L., Ikegami, M., Shannon, J. M., and Weaver, T. E. (2002) Maintenance of the mouse type II cell phenotype *in vitro*. *Am. J. Physiol. Lung Cell. Mol. Physiol.* **283,** L256–L264
24. Huang da, W., Sherman, B. T., and Lempicki, R. A. (2009) Systematic and integrative analysis of large gene lists using DAVID bioinformatics resources. *Nat. Protoc.* **4,** 44–57
25. Ridsdale, R., and Post, M. (2004) Surfactant lipid synthesis and lamellar body formation in glycogen-laden type II cells. *Am. J. Physiol. Lung Cell. Mol. Physiol.* **287,** L743–L751
26. Nogee, L. M., Garnier, G., Dietz, H. C., Singer, L., Murphy, A. M., deMello, D. E., and Colten, H. R. (1994) A mutation in the surfactant protein B gene responsible for fatal neonatal respiratory disease in multiple kindreds. *J. Clin. Invest.* **93,** 1860–1863
27. Nogee, L. M., Dunbar, A. E., 3rd, Wert, S. E., Askin, F., Hamvas, A., and Whitsett, J. A. (2001) A mutation in the surfactant protein C gene associated with familial interstitial lung disease. *N. Engl. J. Med.* **344,** 573–579
28. Clark, J. C., Wert, S. E., Bachurski, C. J., Stahlman, M. T., Stripp, B. R., Weaver, T. E., and Whitsett, J. A. (1995) Targeted disruption of the surfactant protein B gene disrupts surfactant homeostasis, causing respiratory failure in newborn mice. *Proc. Natl. Acad. Sci. U.S.A.* **92,** 7794–7798
29. Shulenin, S., Nogee, L. M., Annilo, T., Wert, S. E., Whitsett, J. A., and Dean, M. (2004) ABCA3 gene mutations in newborns with fatal surfactant deficiency. *N. Engl. J. Med.* **350,** 1296–1303
30. Ramirez, M. I., Millien, G., Hinds, A., Cao, Y., Seldin, D. C., and Williams, M. C. (2003) T1α, a lung type I cell differentiation gene, is required for normal lung cell proliferation and alveolus formation at birth. *Dev. Biol.* **256,** 61–72
31. Bassères, D. S., Levantini, E., Ji, H., Monti, S., Elf, S., Dayaram, T., Fenyus, M., Kocher, O., Golub, T., Wong, K. K., Halmos, B., and Tenen, D. G. (2006) Respiratory failure due to differentiation arrest and expansion of alveolar cells following lung-specific loss of the transcription factor C/EBPα in mice. *Mol. Cell Biol.* **26,** 1109–1123
32. Pepicelli, C. V., Lewis, P. M., and McMahon, A. P. (1998) Sonic hedgehog regulates branching morphogenesis in the mammalian lung. *Curr. Biol.* **8,** 1083–1086
33. Goss, A. M., Tian, Y., Tsukiyama, T., Cohen, E. D., Zhou, D., Lu, M. M., Yamaguchi, T. P., and Morrisey, E. E. (2009) Wnt2/2b and β-catenin signaling are necessary and sufficient to specify lung progenitors in the foregut. *Dev. Cell* **17,** 290–298
34. Imai, T., Matsuda, K., Shimojima, T., Hashimoto, T., Masuhiro, Y., Kitamoto, T., Sugita, A., Suzuki, K., Matsumoto, H., Masushige, S., Nogi, Y., Muramatsu, M., Handa, H., and Kato, S. (1997) ERC-55, a binding protein for the papilloma virus E6 oncoprotein, specifically interacts with vitamin D receptor among nuclear receptors. *Biochem. Biophys. Res. Commun.* **233,** 765–769
35. Kling, D. E., Lorenzo, H. K., Trbovich, A. M., Kinane, T. B., Donahoe, P. K., and Schnitzer, J. J. (2002) MEK-1/2 inhibition reduces branching morphogenesis and causes mesenchymal cell apoptosis in fetal rat lungs. *Am. J. Physiol. Lung Cell. Mol. Physiol.* **282,** L370–L378
36. Wang, J., Ito, T., Udaka, N., Okudela, K., Yazawa, T., and Kitamura, H. (2005) PI3K-AKT pathway mediates growth and survival signals during development of fetal mouse lung. *Tissue Cell* **37,** 25–35
37. Li, F. F., Shen, J., Shen, H. J., Zhang, X., Cao, R., Zhang, Y., Qui, Q., Lin, X. X., Xie, Y. C., Zhang, L. H., Jia, Y. L., Dong, X. W., Jiang, J. X., Bao, M. J., Zhang, S., Ma, W. J., Wu, X. M., Shen, H., Xie, Q. M., and Ke, Y. (2012) Shp2 plays an important role in acute cigarette smoke-mediated lung inflammation. *J. Immunol.* **189,** 3159–3167
38. Zhang, X., Zhang, Y., Tao, B., Teng, L., Li, Y., Cao, R., Gui, Q., Ye, M., Mou, X., Cheng, H., Hu, H., Zhou, R., Wu, X., Xie, Q., Ning, W., Lai, M., Shen, H., Feng, G. S., and Ke, Y. (2012) Loss of Shp2 in alveoli epithelia induces deregulated surfactant homeostasis, resulting in spontaneous pulmonary fibrosis. *FASEB J.* **26,** 2338–2350

39. Whitsett, J. A., Wert, S. E., and Trapnell, B. C. (2004) Genetic disorders influencing lung formation and function at birth. *Hum. Mol. Genet.* **13,** R207–R215

40. Wan, H., Xu, Y., Ikegami, M., Stahlman, M. T., Kaestner, K. H., Ang, S. L., and Whitsett, J. A. (2004) Foxa2 is required for transition to air breathing at birth. *Proc. Natl. Acad. Sci. U.S.A.* **101,** 14449–14454

41. Cole, T. J., Solomon, N. M., Van Driel, R., Monk, J. A., Bird, D., Richardson, S. J., Dilley, R. J., and Hooper, S. B. (2004) Altered epithelial cell proportions in the fetal lung of glucocorticoid receptor null mice. *Am. J. Respir. Cell Mol. Biol.* **30,** 613–619

42. Yamamoto, H., Yun, E. J., Gerber, H. P., Ferrara, N., Whitsett, J. A., and Vu, T. H. (2007) Epithelial-vascular cross-talk mediated by VEGF-A and HGF signaling directs primary septae formation during distal lung morphogenesis. *Dev. Biol.* **308,** 44–53

43. Whitsett, J. A., Clark, J. C., Picard, L., Tichelaar, J. W., Wert, S. E., Itoh, N., Perl, A. K., and Stahlman, M. T. (2002) Fibroblast growth factor 18 influences proximal programming during lung morphogenesis. *J. Biol. Chem.* **277,** 22743–22749

44. Wan, H., Luo, F., Wert, S. E., Zhang, L., Xu, Y., Ikegami, M., Maeda, Y., Bell, S. M., and Whitsett, J. A. (2008) Kruppel-like factor 5 is required for perinatal lung morphogenesis and function. *Development* **135,** 2563–2572